



# Dependence of the probability of escape on the Jacobi constant in the $N$ -body ring problem without central body

Ibrahim Belgharbi, Juan F. Navarro<sup>a</sup>

Department of Applied Mathematics, University of Alicante, Alicante, Spain

Received: 9 November 2022 / Accepted: 15 March 2023  
© The Author(s) 2023

**Abstract** In this work, we perform a numerical exploration of the escape in the  $N$ -body ring problem in absence of a central body, for  $4 \leq N \leq 9$  and ten values of the Jacobi constant. We show how the probability of escape per interval of time varies as a function of the Jacobi constant, finding that, for values of the Jacobi constant smaller than a certain limit value, the probability of escape from the system tends to decrease with time. However, if we consider values of the Jacobi constant larger than this limit value, the probability of escape grows with time, for times of escape smaller than 100 units of time.

## 1 Introduction

The problem of  $N$  bodies dates back to the work of ancient Greek astronomers and is the key to understanding the motion of celestial bodies. Nowadays, this problem has sparked a great deal of interest in many research groups since the irruption of computers and, after that, the development of numerical methods especially adapted to celestial mechanics problems. The  $N$ -body problem describes the motion of  $N$  bodies of arbitrary masses and initial conditions interacting through Newton's law of gravitation. As it is not possible to give the general solution to the  $N$ -body problem, the determination of particular solutions where the  $N$  mass points fulfill certain initial conditions has a great importance. This is the case of homographic solutions, that is, solutions such that the configuration of the  $N$  bodies of the system remains similar when time changes. Two  $N$ -body configurations are similar if we can pass from one to the other by means of a rotation or a dilatation. Euler found three collinear homographic solutions in the three-body problem [1] and, in 1772, Lagrange [2] found two additional solutions, where the bodies are located at the vertices of an equilateral triangle.

Simó [3] defines a choreography as a solution of the  $N$ -body problem for which all the bodies describe a periodic motion along the same fixed curve, without colliding and with a constant phase shift. Chenciner and Montgomery [4] found the first choreography for the three-body problem after the equilateral solution of Lagrange. The configuration of  $N$  bodies axisymmetrically arranged along a circumference is an extension of the Lagrange solution for the three-body problem to the  $N$ -body problem, and this is the object of study of this paper. Other authors have devoted their work to investigate choreographies of  $N$  bodies moving around  $n$  concentric circular orbits, where each circular orbit contains  $m$  axisymmetrically located bodies with equal masses, and the whole structure rotates around its symmetry axis. These structures can be treated as systems formed by mutually embedded polygons rotating at a constant angular velocity [5, 6]. Likewise, Llibre and Mello [7] have analyzed the existence of families of triple or quadruple nested planar central configurations for the  $N$ -body problem, for  $N = 6, 8, 9$ .

In this paper, we focus on a special case of the so-called  $N$ -body ring problem, which models a wide variety of astronomical systems, as the motion of co-orbital satellites or planetary rings. This problem deals with the motion of an infinitesimal particle under the gravitational influence of a ring of  $N$  equally spaced bodies of equal masses, moving with the same mean motion around a primary located at the center of the configuration. Maxwell analyzed this problem for the first time in 1859 [8], when he tackled the problem of studying the stability of the rings of Saturn. Salo and Yoder [9] showed that this configuration is locally unstable for  $N \leq 6$ , and locally stable for  $N \geq 7$ . They also proved that the ring configuration is the only stationary configuration when  $N \geq 9$ . The work developed in this field by Kalvouridis is also of great interest. In [10], Kalvouridis reports the main results of his research concerning the existence of periodic orbits for  $N > 7$ , and considering several values of the mass ratio, showing the distribution of these orbits in the configuration space of initial conditions. In [11], Kalvouridis gives a detailed overview of the results obtained on the topic between the years 1997 and 2008.

The problem of escaping particles from open Hamiltonian systems is one of the most analyzed topics in nonlinear dynamics [12–25]. In this kind of systems, there exists a finite energy of escape,  $E_e$ , such that if the energy of the particle is smaller than  $E_e$ , the equipotential surfaces are closed and the escape from the system is impossible. However, for values of the energy larger

<sup>a</sup> e-mail: [jf.navarro@ua.es](mailto:jf.navarro@ua.es) (corresponding author)

than  $E_e$ , these surfaces open and several apertures emerge, making possible the escape to infinity. In the last few years, the authors have started a numerical exploration of the escape of a particle from  $N$ -body ring configurations [15, 22]. Recently, in a previous work, Belgharbi and Navarro [15] perform a numerical analysis to study how the central mass to peripheral mass ratio affects the distribution of times of escape for  $N = 4$ , finding a sequential pattern in the evolution of the probability of escape per interval of time. Also, Navarro and Martínez-Belda [26] have determined the basins of escape from the  $N$ -body ring configuration, for  $5 \leq N \leq 8$ , analyzing the percentage of escaping orbits, as well as the way the escape is distributed among the different openings of the potential well.

In this paper, we analyze how the probability of escape per interval of time depends on the Jacobi constant  $C$  in the  $N$ -body ring configuration in the absence of a central body, that is, when we consider the value of the mass ratio equal to zero. We have performed this study for  $4 \leq N \leq 9$ . For the sake of simplicity, let us introduce here the set  $\mathbb{N}_{4,9} = \{4, 5, 6, 7, 8, 9\}$ . For each  $N \in \mathbb{N}_{4,9}$ , we have taken ten values of the Jacobi constant for the purpose of sketching the evolution of the probability of escape with respect to the value of  $C$ . Then, we have defined grids of  $2^9 \times 2^9$  initial conditions on the surface of section defined by  $x = y, \dot{y} > 0$ . Each initial condition on the grid has been integrated up to  $T_{\max} = 100$  units of time, to focus on short times of escape, as they are related with the geometry of the first intersections of the set of ingoing asymptotic trajectories to the Lyapunov orbits located at the apertures of the potential well. These structures are in charge of regulating the escape from the system.

The results of our work indicate that there exists a value of the Jacobi constant, denoted by  $C_{N,H}$ , for which, on average, the probability of escape per interval of time remains constant with respect to time. If the Jacobi constant is smaller than  $C_{N,H}$ , the probability of escape per interval of time decreases with time. However, when the Jacobi constant has a value between  $C_{N,H}$  and the critical value, the probability of escape per interval of time increases with time, at least for times of escape below 100 units of time.

## 2 Equations of motion and curves of zero velocity

The equations of motion of the  $N$ -body ring problem without central body are well known and have been described in many works [10, 11, 15, 26]. This problem deals with the motion of a point particle under the Newtonian influence of a configuration of  $N$  bodies (called primaries) with the same mass distributed on a circumference occupying the vertices of a regular polygon of  $N$  sides. These primaries rotate at a constant angular velocity around the center of the circumference. If we consider a barycentric synodic coordinate system  $Oxyz$  rotating with the primaries, the equations of motion are given by

$$\ddot{x} - 2\dot{y} = \frac{\partial U}{\partial x}, \quad \ddot{y} + 2\dot{x} = \frac{\partial U}{\partial y}, \tag{1}$$

where the potential  $U(x, y)$  reads

$$U(x, y) = \frac{1}{2}(x^2 + y^2) + \frac{1}{\Delta} \sum_{v=1}^N \frac{1}{r_v(x, y)},$$

$r_v$  are the distances between the point particle and the primaries, for  $v = 1, \dots, N$ , and  $\Delta$  is given by

$$\Delta = M \Lambda,$$

being

$$\Lambda = \sum_{v=2}^N \frac{\sin^2 \theta \cos((N/2 + 1 - v)\theta)}{\sin^2((N + 1 - v)\theta)} = \sum_{v=2}^N \frac{\sin^2 \theta}{\sin((v - 1)\theta)},$$

and

$$M = \sqrt{2(1 - \cos \psi)} = 2 \sin \theta.$$

In these formulas,  $\psi$  is the angle between the center of mass of the system and two successive peripheral primaries, and  $\theta = \psi/2 = \pi/N$ . In the process of obtaining the equations of motion, dimensionless quantities  $x_v, y_v$  and  $t$  are introduced by transforming the physical ones ( $x'_v, y'_v$  and  $t'$ ) by means of the following relations [27]:

$$x_v = x'_v/\alpha, \quad y_v = y'_v/\alpha$$

and

$$t = \omega t',$$

for any  $v = 1, \dots, N$ , where  $x'_v$  and  $y'_v$  denote the coordinates of the primaries in the barycentric synodic frame,  $\alpha$  is the distance between two successive primaries and  $\omega$  is the constant angular velocity of the primaries. Thus, time is measured in terms of the period of motion of the primaries.

**Table 1**  $C_{N,e}$ , for  $N \in \mathbb{N}_{4,9}$

$N$	$C_{N,e}$
4	4.298576
5	5.633254
6	7.262526
7	9.154474
8	11.294434
9	13.673839

**Table 2**  $C_{N,1}$ , for  $N \in \mathbb{N}_{4,9}$

$N$	$C_{N,1}$
4	4.280
5	5.615
6	7.244
7	9.136
8	11.276
9	13.655

This system has a first integral, known as Jacobi constant, given by

$$C = 2U(x, y) - (\dot{x}^2 + \dot{y}^2). \tag{2}$$

As  $\dot{x}^2 + \dot{y}^2 = 2U(x, y) - C$  must be a positive quantity, the curves defined by  $C - 2U(x, y) = 0$  determine the boundary of the region where the motion can take place.

In this work, we take  $N \in \mathbb{N}_{4,9}$  and, for each of these values of  $N$ , ten values of the Jacobi constant  $C$ . It is well known that there exists a value of the Jacobi constant depending on  $N$ , known as its critical value and denoted by  $C_{N,e}$ , for which the curves of zero velocity open [22]. Thus, for values of the Jacobi constant smaller than the critical  $C_{N,e}$ , particles may exit from the system through one of the apertures of the potential well. Each of the  $N$  openings of the curves of zero velocity is guarded by a periodic orbit called Lyapunov orbit (LO). If a particle crosses one of the LO from the central part to the outside of the configuration, we consider that the particle leaves the potential well and escapes from the system. The time of escape  $t_{\text{esc}}$  of an initial condition is defined as the time the corresponding trajectory needs to cross one of the LO with its velocity heading out of the potential well. In Table 1, we give the critical values of the Jacobi constant, for any  $N \in \mathbb{N}_{4,9}$ .

In our analysis, the values of the Jacobi constant have been chosen so that the size of the corresponding opening of the potential well is approximately of the same size for any  $N \in \mathbb{N}_{4,9}$ . We have denoted these sets of values by  $C_{N,\nu}$ , for any  $N \in \mathbb{N}_{4,9}$  and  $\nu = 1, \dots, 10$ , and are given by

$$C_{N,\nu} = C_{N,1} + h(\nu - 1), \quad \nu = 1, \dots, 10,$$

where  $h = 2 \times 10^{-3}$ , and  $C_{N,1}$ , corresponding to the biggest size of the apertures, are given in Table 2, for any  $N \in \mathbb{N}_{4,9}$ .

In Figs. 1 and 2, we show the curves of zero velocity of the system for  $N = 4, 5, 6$  (Fig. 1) and  $N = 7, 8, 9$  (Fig. 2). In the first and second row of both figures, we depict these curves for the values of the Jacobi constant corresponding to the smallest and biggest opening of the potential well, respectively. Thus, in Fig. 1, we show the curves of zero velocity for  $N = 4, C_{4,10} = 4.298$  (left upper panel),  $N = 4, C_{4,1} = 4.280$  (left lower panel),  $N = 5, C_{5,10} = 5.633$  (middle upper panel),  $N = 5, C_{5,1} = 5.615$  (middle lower panel),  $N = 6, C_{6,10} = 7.262$  (right upper panel) and  $N = 6, C_{6,1} = 7.244$  (right lower panel). In Fig. 2, we show the curves of zero velocity for  $N = 7, C_{7,10} = 9.154$  (left upper panel),  $N = 7, C_{7,1} = 9.136$  (left lower panel),  $N = 8, C_{8,10} = 11.294$  (middle upper panel),  $N = 8, C_{8,1} = 11.276$  (middle lower panel),  $N = 9, C_{9,10} = 13.673$  (right upper panel) and  $N = 9, C_{9,1} = 13.655$  (right lower panel).

### 3 Numerical exploration

The numerical analysis of the escape in this system is performed on the surface of section defined by  $y = x, \dot{y} > 0$ . For each of the values of  $N$  and  $C$  described in the previous section, we consider a set  $S_{N,C}$  of  $2^9 \times 2^9$  initial conditions distributed evenly in the  $(x, \dot{x})$  space, and conditioned by the value of the Jacobi constant. If  $(x_0, \dot{x}_0)$  are known, we set  $y_0 = x_0$  and, then,  $\dot{y}_0$  is determined using the relation

$$\dot{y}_0 = +\sqrt{2U(x_0, y_0) - C - \dot{x}_0^2}.$$

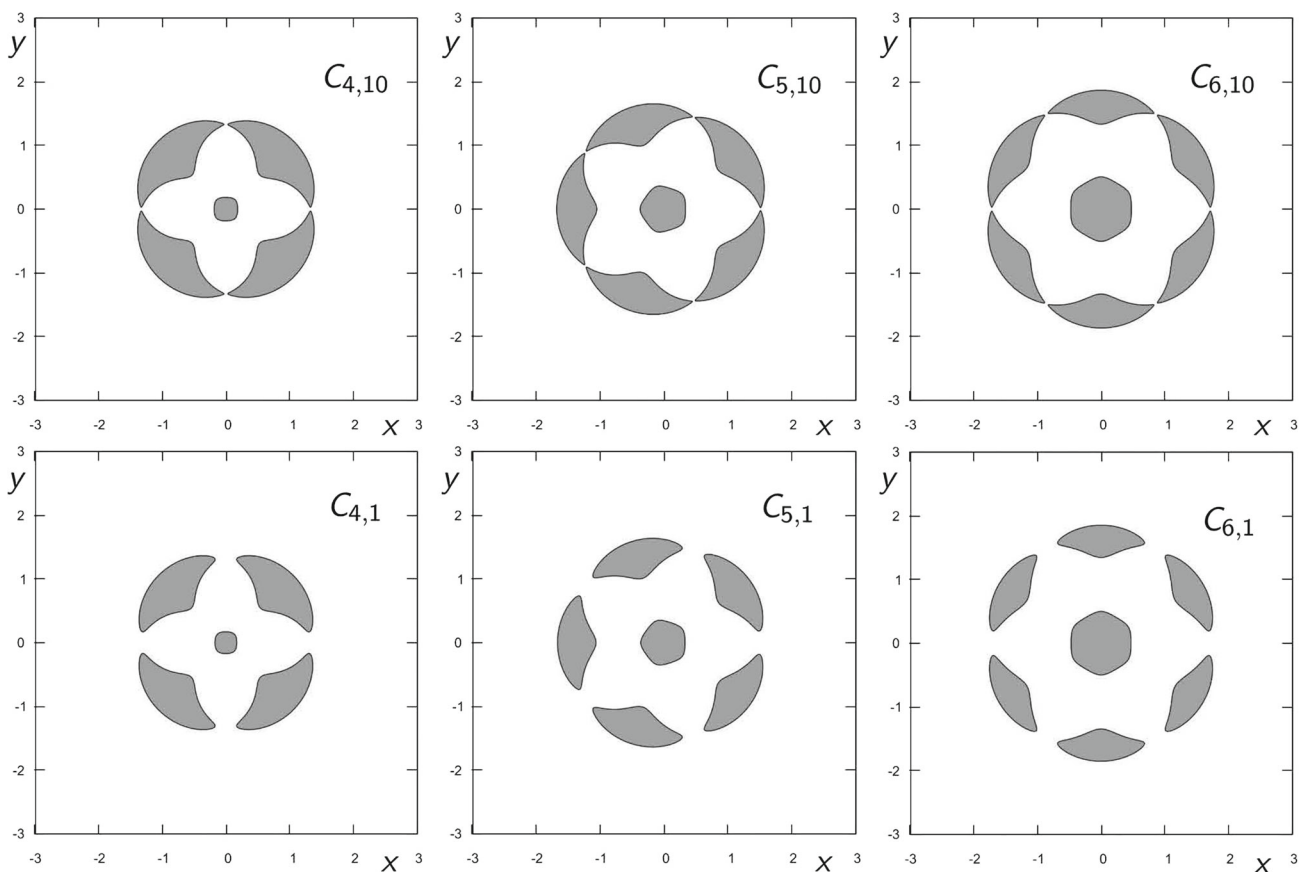


**Fig. 1** Curves of zero velocity for  $N = 4, 5, 6$ , and a pair of values of Jacobi constant related to the smallest (upper panel) and biggest (lower panel) size of the openings of the potential well

Thus, we take the initial conditions in the set  $D_{N,C}$  defined by

$$D_{N,C} = \{(x_0, \dot{x}_0) \in \mathbb{R}^2 : 2U(x_0, x_0) - C - \dot{x}_0^2 \geq 0\}. \tag{3}$$

To perform an analysis of the escape in this problem, we integrate each of the initial conditions in the grid  $S_{N,C}$  contained in  $D_{N,C}$  numerically up to a maximum time of  $T_{\max} = 10^2$  [26].

The relation between the escape of a particle from an open Hamiltonian system and the location of its initial condition with respect to the stable manifolds of the Lyapunov orbits guarding the apertures of the curves of zero velocity of the system is well known [19, 21, 28, 29]. If the initial condition of the orbit belongs to the interior of the hyper-surface defined by the stable manifold of any of the Lyapunov orbits, then the orbit will leave the system by crossing the corresponding Lyapunov orbit. If we consider an initial condition in a certain surface of section, the orbit will leave the potential well without crossing again the surface of section if the initial condition belongs to the region delimited by the first intersection between the surface of section and the stable manifold of any of the Lyapunov orbits of the system. In general, if the initial condition of the orbit belongs to the region delimited by the  $\nu$ -th intersection between the surface of section and the stable manifold of any of the Lyapunov orbits, the particle will leave the system through the corresponding aperture of the potential well after intersecting  $\nu - 1$  times the surface of section. Thus, the limiting curves of the basins of escape of the system are determined by the projection of the stable manifolds of the Lyapunov orbits located at the apertures of the potential well. The first intersections between these hyper-surfaces and the surface of section have a simple geometry. But the structure of these intersections becomes more complex as the number of the intersections grows [19]. Likewise, the area of the region enclosed by these limiting curves decays very quickly with the number of the intersections and, so, the same happens with the amount of orbits that escape from the system [22]. Consequently, in order to unveil how these structures are located on the surface of section, we have focused on the analysis of times of escape smaller than  $T_{\max}$ .

For the numerical integration of the equations of motion, we have used the method of recurrent power series adapted to the  $N$ -body ring problem. This method converges for any initial condition not leading to a binary collision [30]. In our computations, we have set the number of the term series to 21 and fixed the accuracy of the method to  $\epsilon = 10^{-18}$  in order to determine the variable step size.

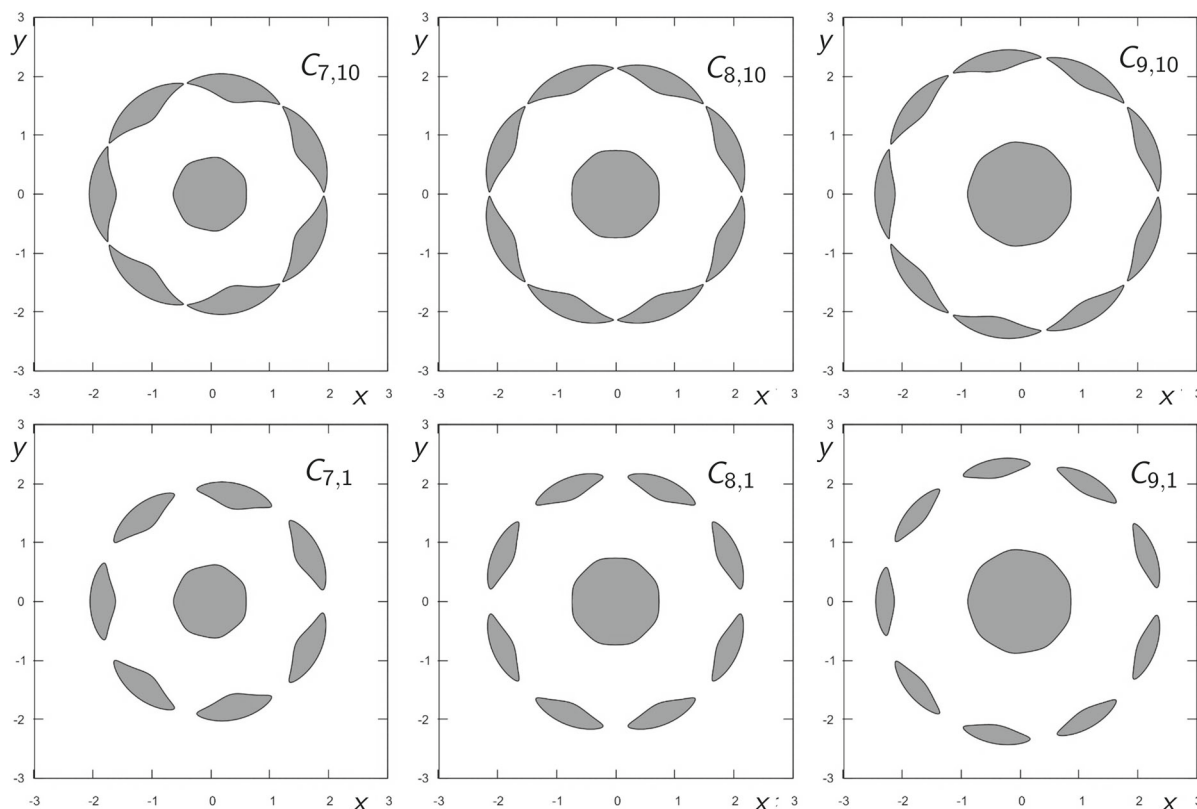


**Fig. 2** Curves of zero velocity for  $N = 7, 8, 9$ , and a pair of values of Jacobi constant related to the smallest (upper panel) and biggest (lower panel) size of the openings of the potential well

Now, let us define some quantities that we will use in the paper.  $M(N, C)$  denotes the total number of initial conditions of  $S_{N,C}$  belonging to the domain  $D_{N,C}$ , being  $N$  and  $C$  the number of primaries and the value of the Jacobi constant, respectively.  $E(N, C)$  denotes the total number of initial conditions in  $S_{N,C} \cap D_{N,C}$  corresponding to orbits that escape from the system with a time of escape smaller than  $T_{max}$ ,  $E(N, C, t_1, t_2)$  denotes the number of initial conditions in  $S_{N,C} \cap D_{N,C}$  corresponding to orbits that escape with a time of escape  $t$  such that  $t_1 < t \leq t_2$ . Also,  $E(N, C, t) = E(N, C, 0, t)$  is the number of initial conditions corresponding to trajectories that leave the system in a time not larger than  $t$ .  $P(N, C, t_1, t_2)$  refers to the probability of escape from the system in a time  $t$  such that  $t_1 < t \leq t_2$ ,  $P(N, C, t) = P(N, C, 0, t)$  and  $P(N, C) = P(N, C, T_{max})$ . These quantities are defined by

$$P(N, C, t_1, t_2) = \frac{E(N, C, t_1, t_2)}{M(N, C)}, \quad P(N, C, t) = \frac{E(N, C, t)}{M(N, C)},$$

and

$$P(N, C) = \frac{E(N, C, T_{max})}{M(N, C)}.$$

With the aim of carrying out the analysis of the influence of the Jacobi constant on the probability of escape per interval of time, we have calculated  $P(4, C_{4,v}, t_1, t_2)$ ,  $P(5, C_{5,v}, t_1, t_2)$ ,  $P(6, C_{6,v}, t_1, t_2)$ ,  $P(7, C_{7,v}, t_1, t_2)$ ,  $P(8, C_{8,v}, t_1, t_2)$  and  $P(9, C_{9,v}, t_1, t_2)$ , for  $v = 1, \dots, 10$ ,  $t_1 = nh$ ,  $t_2 = (n + 1)h$ , being  $h = 1$  and  $n \in \mathbb{N}$ ,  $0 \leq n \leq 99$ .

In Fig. 3, we show the probability of escape per interval of time for  $N = 4$ ,  $P(4, C_{4,v}, t_1, t_2)$ , considering  $t_2 - t_1 = 1$ , and ten values of the Jacobi constant of the form  $C_{4,v} = C_{4,1} + h(v - 1)$ , with  $h = 0.002$ , and  $C_{4,1} = 4.280$ . We observe that the behavior of  $P(4, C_{4,v}, t_1, t_2)$  reproduces the same scheme for any of the values of the Jacobi constant we have examined. For values of the time of escape smaller than 3 or 4 units of time, no orbit escapes from the system. Then, we find a maximum of the probability of escape per interval of time for times of escape between 3 and 8 units of time, and, right after that, a secondary maximum. Then, the probability of escape per interval of time shows an oscillatory behavior around an average line. Figure 3 unveils that the slope of the average line of the probability of escape per interval of time is negative, for values of the Jacobi constant  $C$  such that  $C_{4,1} \leq C \leq C_{4,8}$ . However, if  $C_{4,9} \leq C \leq C_{4,10}$ , the slope is positive. This means that there exists a value  $C_{4,H}$  of the Jacobi constant such that if  $C_{4,H} < C < C_{4,e}$ , the slope of the average line of the probability of escape per interval of time is positive. Moreover, if  $C < C_{4,H}$ , the slope is negative. We can also conclude that the probability of escape per interval of time decreases as the value of the Jacobi constant grows.

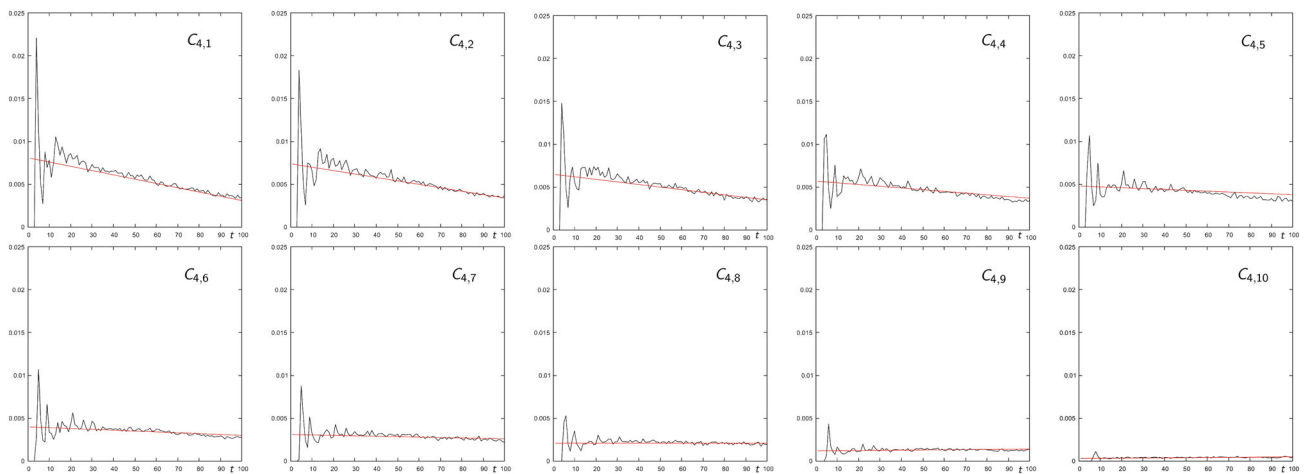


**Fig. 3** Probabilities of escape per interval of time, for values of the Jacobi constant given by  $C_{4,v} = C_{4,1} + h(v - 1)$ ,  $v = 1, \dots, 10$ ,  $h = 2 \times 10^{-3}$ , and  $C_{4,1} = 4.280$

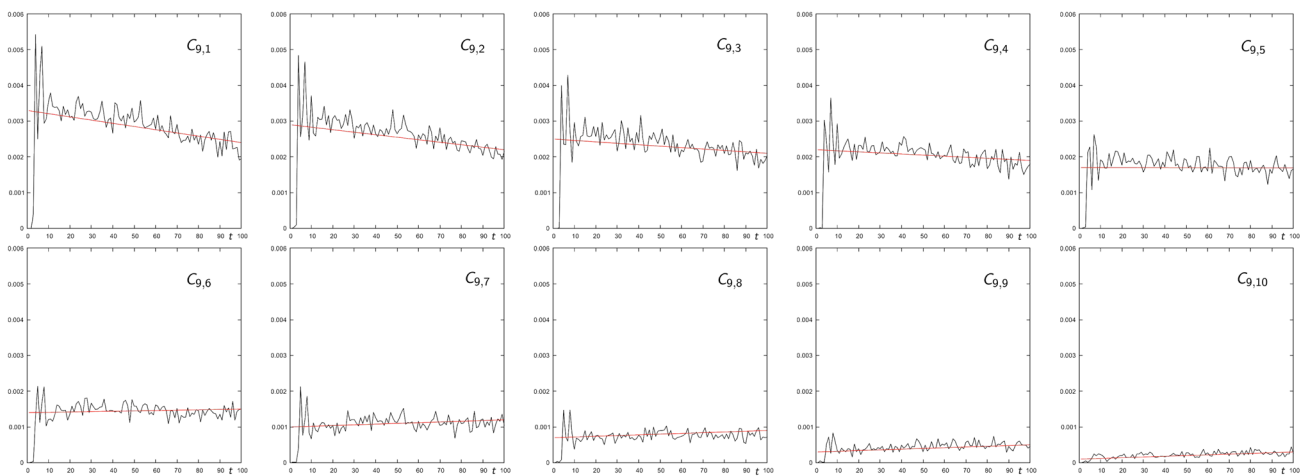


**Fig. 4** Probabilities of escape per interval of time, for values of the Jacobi constant given by  $C_{9,v} = C_{9,1} + h(v - 1)$ ,  $v = 1, \dots, 10$ ,  $h = 2 \times 10^{-3}$ , and  $C_{9,1} = 13.655$

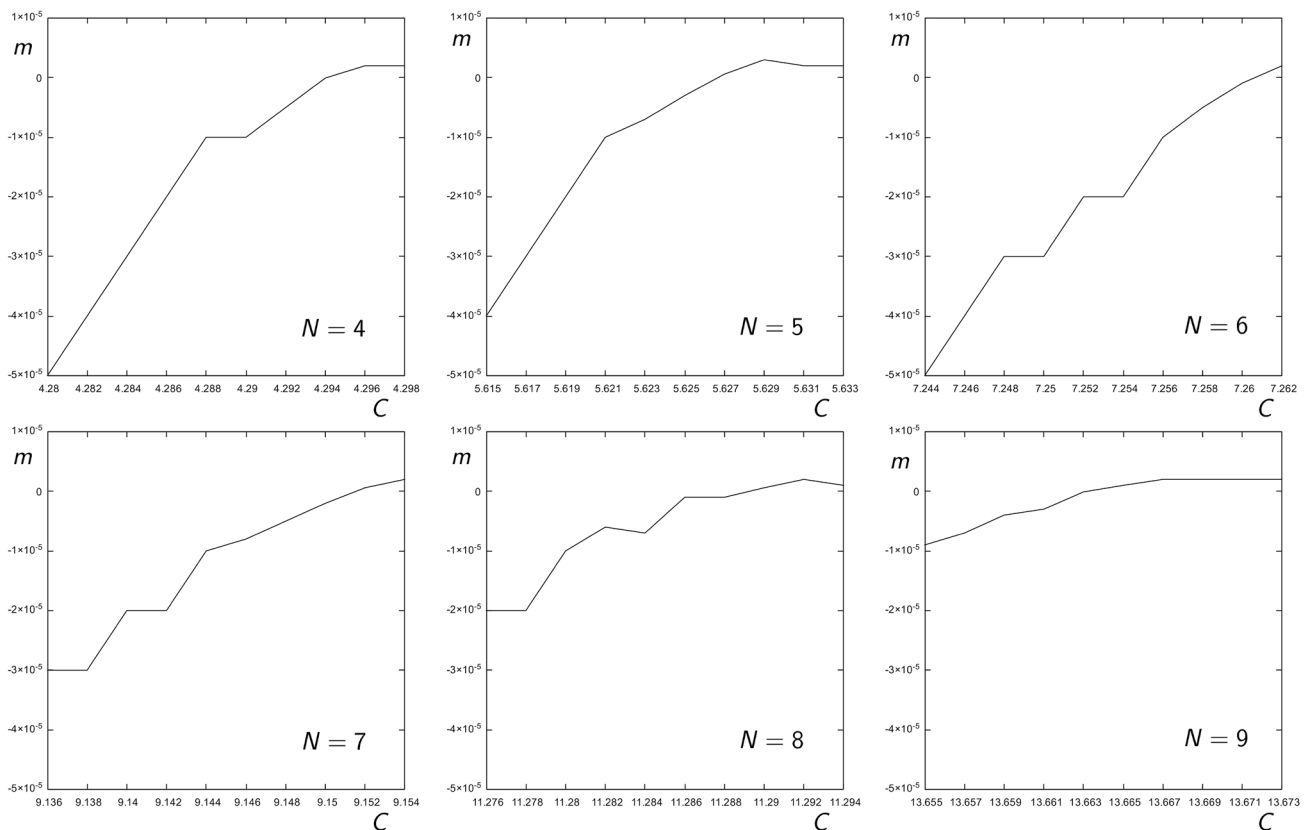
In Fig. 4, we depict the probability of escape per interval of time for  $N = 9$ ,  $P(9, C_{9,v}, t_1, t_2)$ , considering  $t_2 - t_1 = 1$ , and ten values of the Jacobi constant of the form  $C_{9,v} = C_{9,1} + h(v - 1)$ , with  $h = 0.002$ , and  $C_{9,1} = 13.655$ . As before, we find that the behavior of  $P(9, C_{9,v}, t_1, t_2)$  reproduces an analogous pattern to that described for  $N = 4$ , for any of the values of the Jacobi constant we have examined. Thus, again, no orbit escapes from the system with a time of escape smaller than 3 or 4 units of time. Then, we find a pair of main peaks in the probability of escape per interval of time. These pairs of peaks are more or less pronounced depending on the value of the Jacobi constant, but they always exist, except for  $C_{9,10}$ . For times of escape larger than 10 units of time, the probability of escape per interval of time exhibits an oscillatory behavior around an average line. For values of the Jacobi constant  $C$  such that  $C_{9,1} \leq C \leq C_{9,5}$ , the slope of the average line is negative. However, if  $C_{9,6} \leq C \leq C_{9,10}$ , the slope is positive. This means that there exists a value  $C_{9,H}$  of the Jacobi constant such that if  $C_{9,H} < C < C_{9,e}$ , then the slope of the average line of the probability of escape per interval of time is positive. Moreover, if  $C < C_{9,H}$ , the slope is negative. As in the previous case, the probability of escape per interval of time decreases as the value of the Jacobi constant grows. The difference between the two cases we have analyzed,  $N = 4$  and  $N = 9$ , lies in the value of  $C_{N,H}$  and its proximity to  $C_{N,e}$ .

Table 3 shows the slopes of the average lines of the probability of escape per interval of time for  $N = 4$  and  $N = 9$  and the values of the Jacobi constant,  $C_{4,v} = C_{4,1} + h(v - 1)$ ,  $C_{9,v} = C_{9,1} + h(v - 1)$ , with  $h = 0.002$ ,  $C_{4,1} = 4.280$  and  $C_{9,1} = 13.655$ , considering  $T_{\max} = 100$ . The slope of the average line corresponding to  $C_{N,v}$  is denoted by  $m_{N,v}$ , for any  $N \in \mathbb{N}_{4,9}$  and  $v = 1, \dots, 10$ . We notice that as the value of the Jacobi constants  $C_{4,v}$  and  $C_{9,v}$  grows tending to its critical value, the value of the slopes of the average lines also becomes bigger, going from negative to positive.

We have found this same scheme for any  $N \in \mathbb{N}_{4,9}$ . In Fig. 5, we depict the slope of the average line of the probability of escape per interval of time with respect to the value of the Jacobi constant, for any  $N \in \mathbb{N}_{4,9}$ . This figure unveils that the sign of the slope changes independently of the value of the number of primaries we consider. As the value of the Jacobi constant becomes bigger

**Table 3** Jacobi constants and slopes of the average lines of the probability of escape per interval of time, for  $N = 4$  and  $N = 9$

$N = 4$		$N = 9$	
$C_{4,v}$	$m_{4,v}$	$C_{9,v}$	$m_{9,v}$
4.28	$-5 \times 10^{-5}$	13.655	$-9 \times 10^{-6}$
4.282	$-4 \times 10^{-5}$	13.657	$-7 \times 10^{-6}$
4.284	$-3 \times 10^{-5}$	13.659	$-4 \times 10^{-6}$
4.286	$-2 \times 10^{-5}$	13.661	$-3 \times 10^{-6}$
4.288	$-1 \times 10^{-5}$	13.663	$-1 \times 10^{-7}$
4.29	$-1 \times 10^{-5}$	13.665	$1 \times 10^{-6}$
4.292	$-5 \times 10^{-6}$	13.667	$2 \times 10^{-5}$
4.294	$-5 \times 10^{-8}$	13.669	$2 \times 10^{-6}$
4.296	$2 \times 10^{-6}$	13.671	$2 \times 10^{-6}$
4.298	$2 \times 10^{-6}$	13.673	$2 \times 10^{-6}$



**Fig. 5** Slope of the average line of the probability of escape per interval of time versus the Jacobi constant for  $N = 4, 5, 6, 7, 8$  and  $9$

and, then, the size of the openings of the curves of zero velocity becomes smaller, the value of the slope of the average line tends, in general, to increase, going from a negative to a positive value. Thus, there exists a value of the Jacobi constant  $C_{N,H} < C_{N,e}$ , such that the slope of the corresponding average line of the probability of escape per interval of time is equal to zero. Moreover, we notice that the change in the sign of the slope of the average line occurs at a value  $C_{N,H}$  located at a different distance from the critical value  $C_{N,e}$  for any of the values of  $N$  considered. Let us remark here that the value  $C_{N,10}$  is very close to  $C_{N,e}$  and, for values of the Jacobi constant larger than  $C_{N,e}$ , no orbit can escape from the potential well.

In Fig. 6, we show the probability of escape from the system  $P(N, C_{N,v})$  versus the value of the Jacobi constant, for  $N \in \mathbb{N}_{4,9}$ , and considering  $T_{\max} = 100$ . These graphics show that, for any of the values of the number of primaries, the probability of escape decreases when the Jacobi constant grows and, hence, the size of the openings of the curves of zero velocity becomes smaller. Also, we can conclude that  $P(4, C_{4,v}) > P(5, C_{5,v}) > P(6, C_{6,v})$ , and  $P(7, C_{4,v}) > P(8, C_{5,v}) > P(9, C_{6,v})$ , for any  $v = 1, \dots, 10$ . However,  $P(6, C_{6,v}) < P(7, C_{4,v})$ , for any  $v = 1, \dots, 10$ .

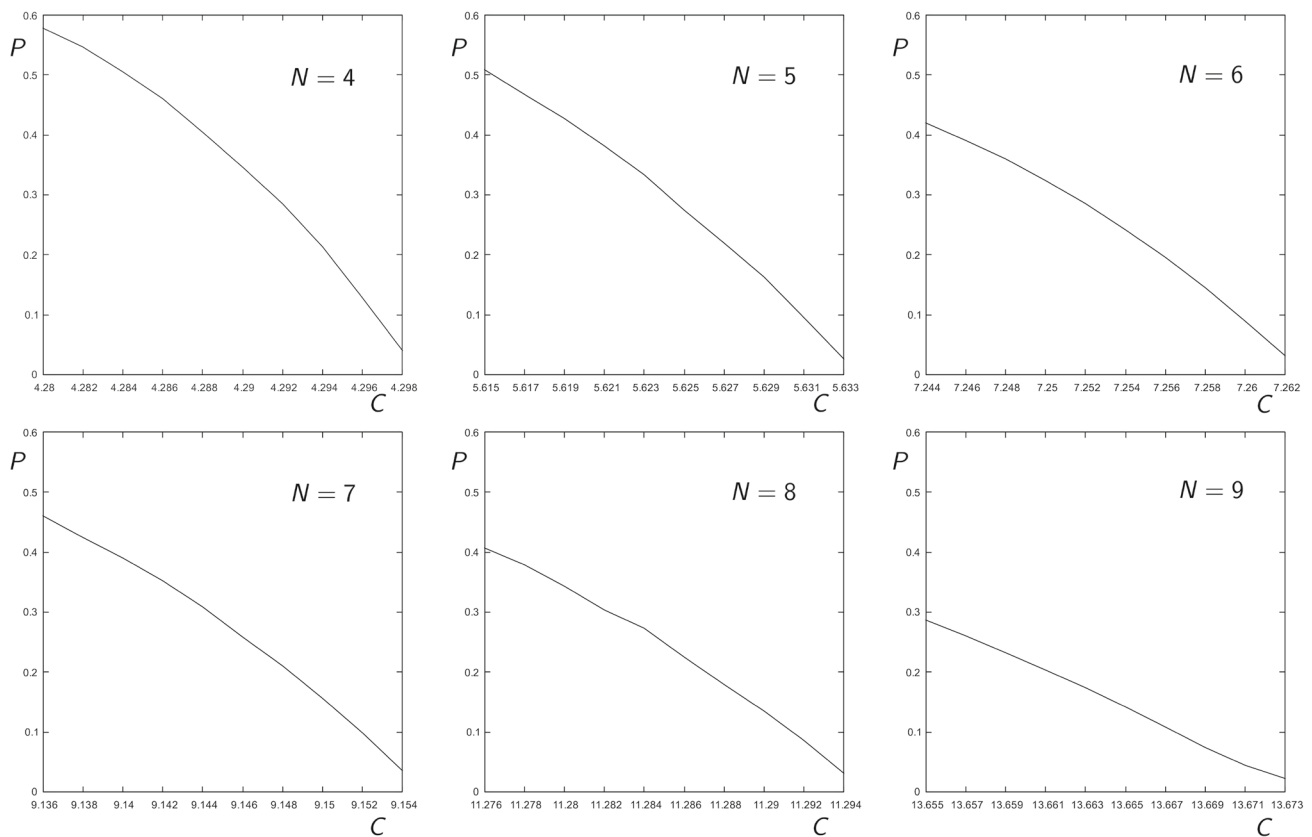


**Fig. 6** Probability of escape  $P(N, C_{N,v})$  versus the value of the Jacobi constant, for  $N = 4, 5, 6, 7, 8$  and  $9$

Navarro and Martínez–Belda [26] found an almost linear relation (with negative slope) between the probability of escape from the system and the number of primaries  $N$ , in the  $N$ -body ring configuration with central body. In this paper, we explore if we find this same linear relation in the absence of a central body. Figure 7 depicts the probability of escape from the system versus the number of primaries  $N$ , for nine of the values of the Jacobi constant we have used in our numerical exploration, and considering  $T_{\max} = 100$ . Each plot corresponds to one value of the Jacobi constant. Thus, in Fig. 7 ( $P(N, C_{N,v})$ ), we depict the probability of escape for  $N = 4, 5, 6, 7, 8, 9$  and the corresponding values of the Jacobi constant,  $C_{N,v}$ . The values of the Jacobi constant employed in each of the plots correspond to apertures of the curves of zero velocity of approximately the same size. We observe that the probability of escape decreases between  $N = 4$  and  $N = 6$ , as well as between  $N = 7$  and  $N = 9$ . However, it always increases between  $N = 6$  and  $N = 7$ . This change in the trend between  $N = 6$  and  $N = 7$  may be the object of a future investigation.

#### 4 Conclusions

In this paper, we have analyzed the dependence of the probability of escape per interval of time on the Jacobi constant in the  $N$ -body ring configuration in the absence of a central body. We have performed this study for  $4 \leq N \leq 9$  and ten values of the Jacobi constant, in order to sketch the evolution of the probability of escape from the system with respect to the value of this constant.

The results obtained through the numerical exploration we have performed indicate that there exists a value of the Jacobi constant, here denoted by  $C_{N,H}$ , such that, on average, the probability of escape per interval of time remains constant, for short times of escape, that is, for times of escape smaller than 100 units of time. If the value of the Jacobi constant is smaller than  $C_{N,H}$ , the probability of escape per interval of time decreases with time. However, for values of the Jacobi constant between  $C_{N,H}$  and the critical value, the probability of escape per interval of time increases with time, at least for times of escape smaller than 100 units of time.

As the value of the Jacobi constant grows and, consequently, the size of the apertures of the curves of zero velocity of the system becomes smaller, so does the number of orbits leaving the system with short times of escape. In some sense, we could say that the path to escape from the system becomes more complicated as the size of the aperture tends to zero. Moreover, the size of the Lyapunov orbit and, so, of the region delimited by the intersection between the stable manifold of this orbit and the surface of section



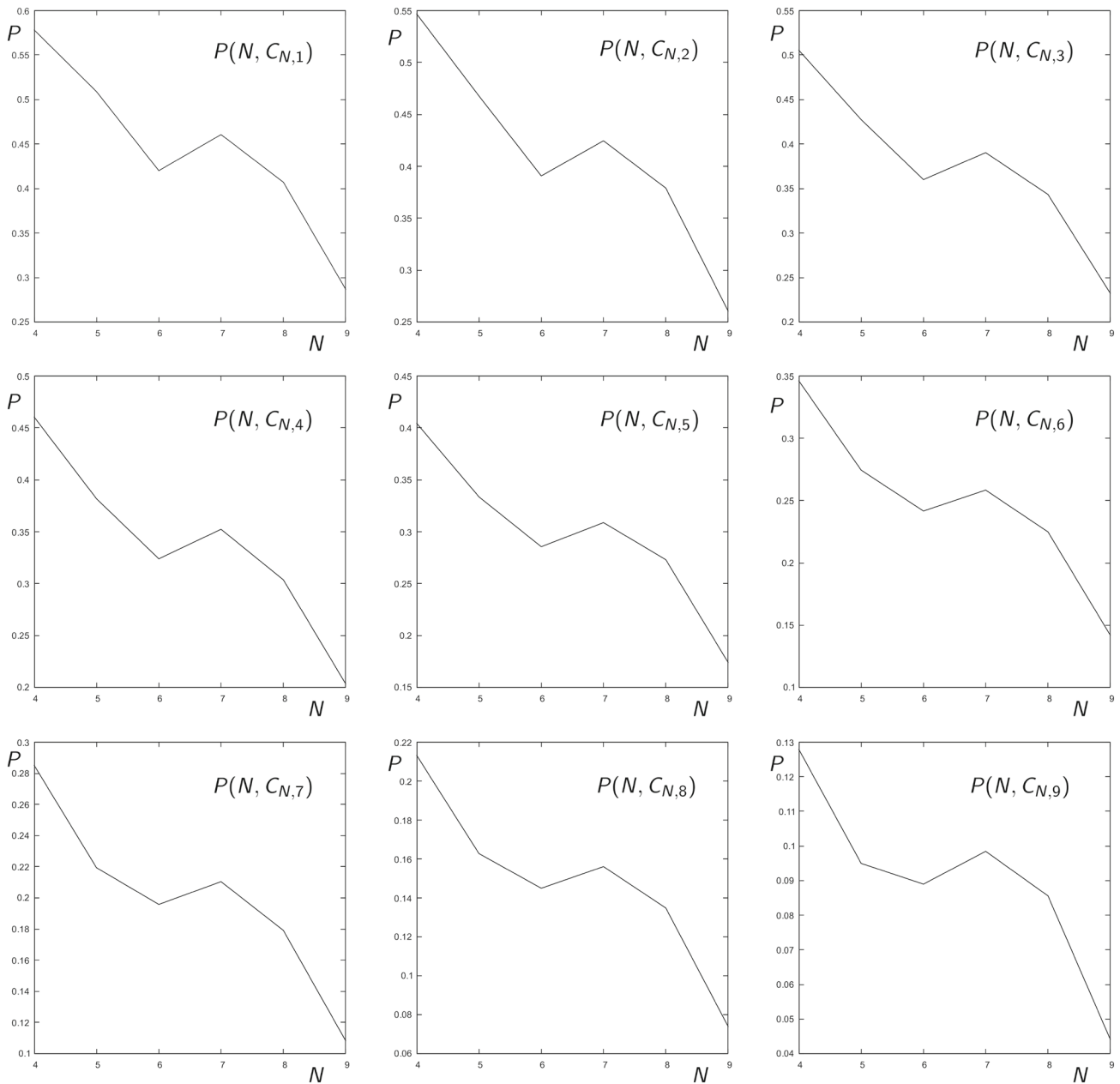


**Fig. 7** Probability of escape  $P(N, C_{N,\nu})$  versus the number of primaries  $N$ , for  $N = 4, 5, 6, 7, 8$  and  $9$

we are considering, is inversely proportional to the value of the Jacobi constant, that is, the Lyapunov orbit becomes smaller as the Jacobi constant tends to  $C_{N,e}$ , as the size of the Lyapunov orbit is directly proportional to the size of the aperture. This fact implies that the number of orbits that escape from the system with short times of escape decreases when the Jacobi constant tends to  $C_{N,e}$  (and the size of the aperture decreases) and, moreover, the orbits that leave the potential well need more time to escape: The size of the aperture is inversely proportional to the average time of escape from the system. This is the reason why we observe a positive slope of the average line of the probability of escape per interval of time for values of  $C$  larger than  $C_{N,H}$ .

We have also found that, if  $N_1 < N_2$ , then  $P(N_1, C_{N_1,\nu}) > P(N_2, C_{N_2,\nu})$ , for any  $\nu = 1, \dots, 10$  corresponding to values of the Jacobi constant related to openings of the curves of zero velocity of approximately the same size, except if  $N_1 = 6$  and  $N_2 = 7$ . A further study is required in order to clarify the behavior of the trend of the probability of escape between these two values of the number of bodies. We think that we will find the clue in the analysis of the way the geometry of the stable manifolds of the Lyapunov orbits changes depending on the value of  $N$ .

**Funding** Open Access funding provided thanks to the CRUE-CSIC agreement with Springer Nature.

**Data Availability Statement** This manuscript has associated data in a data repository. [Authors' comment: We can provide the data sets generated during the research on reasonable request.]

## Declarations

**Conflict of interest** This work does not have any conflicts of interest.

**Open Access** This article is licensed under a Creative Commons Attribution 4.0 International License, which permits use, sharing, adaptation, distribution and reproduction in any medium or format, as long as you give appropriate credit to the original author(s) and the source, provide a link to the Creative Commons licence, and indicate if changes were made. The images or other third party material in this article are included in the article's Creative Commons licence, unless indicated otherwise in a credit line to the material. If material is not included in the article's Creative Commons licence and your intended use is not permitted by statutory regulation or exceeds the permitted use, you will need to obtain permission directly from the copyright holder. To view a copy of this licence, visit <http://creativecommons.org/licenses/by/4.0/>.

## References

1. L. Euler, De moto rectilineo trium corporum se mutuo attrahentium. *Novi Comm. Acad. Sci. Imp. Petrop.* **11**, 144–151 (1767)
2. J.L. Lagrange, *Essai sur le problème de trois corps. Ouvres*, vol. 6 (Gauthier-Villars, Paris, 1873)
3. C. Simó, New Families of Solutions in N-Body Problems. In: Casacuberta C., Miró-Roig R. M., Verdera J., Xambó-Descamps S. (eds) European Congress of Mathematics. Progress in Mathematics. Birkhäuser, Basel, 201, 101–115, (2001)
4. A. Chenciner, R. Montgomery, A remarkable periodic solution of the three body problem in the case of equal masses. *Ann. Math.* **152**, 881–901 (2000)
5. E.A. Grebenikov, *Mathematical problems in homographic dynamics* (MAX Press, Moscow, 2010)
6. J.J. Smulsky, Exact solution to the problem of  $N$  bodies forming a multi-layer rotating structure. *SpringerPlus* **4**, 361 (2015)
7. J. Llibre, L.F. Mello, Triple and quadruple nested central configurations for the planar  $n$ -body problem. *Phys. D* **238**, 563–571 (2009)
8. J.C. Maxwell, *On the stability of motions of Saturn's rings* (Macmillan and Company, Cambridge, 1859)
9. H. Salo, C.F. Yoder, The dynamics of coorbital satellite systems. *Astron. Astrophys.* **205**, 309–327 (1988)
10. T.J. Kalvouridis, Particle motions in Maxwell's ring dynamical systems. *Celest. Mech. Dyn. Astr.* **102**, 191–206 (2008)
11. T.J. Kalvouridis, The Ring Problem of  $(N + 1)$  Bodies: An Overview, in *Dynamical systems and methods*. ed. by A.C.J. Luo et al. (Springer, 2009), pp.135–150
12. J. Aguirre, M.A.F. Sanjuan, Limit of small exits in open Hamiltonian systems. *Phys. Rev. E* **67**, 056201 (2003)
13. B. Barbanis, Escape regions of a quartic potential. *Celest. Mech. Dyn. Astron.* **48**(1), 57–77 (1990)
14. R. Barrio, F. Blesa, S. Serrano, Bifurcations and safe regions in open Hamiltonians. *New J. Phys.* **11**, 053004 (2009)
15. I. Belgharbi, J.F. Navarro, Effect of the mass ratio on the escape in the 4-body ring problem. *Eur. Phys. J. Plus* **137**, 850 (2022)
16. G. Contopoulos, Asymptotic curves and escapes in Hamiltonian systems. *Astron. Astrophys.* **231**(1), 41–45 (1990)
17. G. Contopoulos, K. Efstathiou, Escapes and recurrence in a simple Hamiltonian system. *Celest. Mech. Dyn. Astron.* **88**, 163–183 (2004)
18. G. Contopoulos, D. Kaufmann, Types of escapes in a simple Hamiltonian system. *Astron Astrophys* **253**, 379–388 (1992)
19. J.F. Navarro, On the escape from potentials with two exit channels. *Sci. Rep.* **9**, 13174 (2019)
20. J.F. Navarro, Dependence of the escape from an axially symmetric galaxy on the energy. *Sci. Rep.* **11**, 8427 (2021)
21. J.F. Navarro, J. Henrard, Spiral windows for escaping stars. *Astron. Astrophys.* **369**, 1112–1121 (2001)
22. J.F. Navarro, I. Belgharbi, M.C. Martínez-Belda, Analysis of the escape in systems with four exits channels. *Math. Meth. Appl. Sci.* **46**, 1032–1044 (2023)
23. C. Siopsis, H.E. Kandrup, G. Contopoulos, R. Dvorak, Universal properties of escape in dynamical systems. *Celest. Mech. Dyn. Astron.* **65**(1–2), 57–68 (1996)
24. E.E. Zotos, A Hamiltonian system of three degrees of freedom with eight channels of escape: the great escape. *Nonlinear Dyn.* **76**, 1301–1326 (2014)
25. E.E. Zotos, Escape dynamics in a Hamiltonian system with four exit channels. *Nonlinear Stud* **22**(3), 433–452 (2015)
26. J.F. Navarro, M.C. Martínez-Belda, Analysis of the distribution of times of escape in the  $N$ -body ring problem. *J. Comput. Appl. Math.* **404**, 113396 (2021)
27. T.J. Kalvouridis, A planar case of the  $n + 1$  body problem: the ring problem. *Astrophys Space Sci* **260**, 309–325 (1999)
28. G. Gómez, W.S. Koon, M.W. Lo, J.E. Marsden, J. Masdemont, S.D. Ross, Connecting orbits and invariant manifolds in the spatial restricted three-body problem. *Nonlinearity* **17**, 1571–1606 (2004)
29. W.S. Koon, M.W. Lo, J.E. Marsden, S. Ross, *Dynamical systems, the three-body Problem and space mission design* (Marsden Books, Wellington, 2008)
30. J.F. Navarro, Numerical integration of the  $N$ -body ring problem by recurrent power series. *Celest. Mech. Dyn. Astr.* **30**, 16 (2018)